A Parametric Channel Model for Smart Antennas Incorporating Mobile Station Mobility

Salman Durrani[†]
[†]Department of Engineering,
The Australian National University, Canberra, Australia.
Email: salman.durrani@anu.edu.au

Marek E. Bialkowski[‡]
[‡]School of Information Technology & Electrical Engineering,
The University of Queensland, Brisbane, Australia.
Email: meb@itee.uq.edu.au

***Abstract*— This paper presents a parameterized physical channel model for evaluating the performance of smart antenna systems. The channel model assumes a single antenna at the mobile station and a uniform linear array of omni-directional antenna elements at the base station. It incorporates parameters such as azimuth angle of arrival and departure, angle spread, power delay profiles and Doppler frequency, which have critical influence on the performance of smart antennas. A new feature of the channel model is a thorough framework for the incorporation of user mobility. The proposed model allows for efficient and accurate representation of smart antenna channel aspects, while maintaining low complexity for system level simulations.**

I. Introduction

Smart antennas systems, that employ multiple antennas (array antennas) at the Base Station (BS), are expected to play a key role in future wireless communication systems [1]. By making use of advanced space-time signal processing algorithms, smart antenna systems are able to mitigate interference and improve the capacity and range in wireless systems. A successful adoption of this technology in a given wireless environment requires its extensive testing. In order to minimize the costs associated with this design and development stage, the use of realistic channel models that can accurately characterize spatial as well as temporal variations of the channel is a crucial requirement.

The spatial channel models for smart antennas have received much attention in literature [2], [3]. The channel models for smart antennas can be generally divided into four groups: empirical, deterministic, geometric and physical. Empirical models are based on field measurements [4] while deterministic models use ray-tracing techniques to model the channel impulse response [5]. The advantage of these models is that they provide greater accuracy with site-specific results. However complexity becomes an issue for link-level simulations. Geometric models are defined by a particular distribution of scatterers and assume that the propagation between transmit and receive antennas takes place via scattering from intervening obstacles e.g. Circular Scattering Model (CSM) [6] and Gaussian Scatter Density Model (GDSM) [7]. The main advantage of geometric models is that once the coordinates of the scatterers are drawn from a random process, all necessary spatial information can be easily derived. However the limitations are that only single bounce scattering is considered and the resulting simulation time is large (especially when it is required to generate scatterer distributions for different channel environments). By contrast, physical models use important physical parameters to provide a description of wireless channel characteristics [8]. The main advantage of physical models, compared with scatterer models, is the reduced complexity and easier incorporation of available measurements results as input channel parameters.

An example of physical channel model is the Spatial Channel Model (SCM) proposed by Third Generation Partnership Project Two (3GPP2) [9]. This detailed model is applicable for a variety of environments. However a limitation of the above model for smart antenna applications is that it does not take into account Mobile Station (MS) mobility. Modelling the movement of the MS is crucial as it influences both the spatial and temporal channel characteristics. Also for the case of adaptive beamforming, the smart antenna must track and steer its beam towards the desired user. Therefore, the performance of a smart antenna cannot be realistically evaluated without simulating MS mobility [10]–[12].

In this work, we present a spatio-temporal channel model for use in the performance analysis of wireless communication systems incorporating smart antennas. We extend the SCM model by proposing a thorough framework for the incorporation of MS mobility. The proposed model allows for efficient and accurate characterisation of smart antenna channels while maintaining low complexity for link-level simulations.

This paper is organised as follows. The overall structure of the system and channel model is described in Section II. The novel framework for modelling of mobile station mobility is presented in Section III. The simulation results are discussed in Section IV. Finally conclusions are drawn in Section V.

II. Model Formulation

We consider a single 120° sector with K active users in the system. It is assumed that the BS is an elevated and separate structure that is located well above the surrounding scatterers. Also the BS employs a Uniform Linear Array (ULA) of N omni-directional antenna elements, with inter-element spacing $d = \lambda/2$. The Mobile Station (MS), however, moves on the street level (e.g. at a typical height of $1 - 2$ m) and is surrounded by local scattering structures (e.g., an urban or suburban environment). Furthermore, L dominant and spatially well-separated reflectors (such as hills or large

0-7803-9392-9/06/$20.00 (c) 2006 IEEE

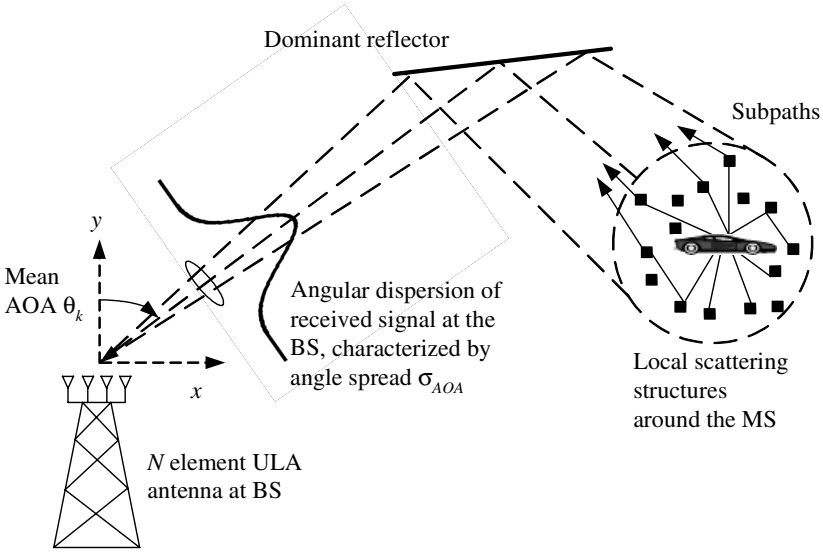

Fig. 1. Smart antenna channel model.

buildings) are located in the environment in the far-field of the array. At each dominant reflector a different combination of the incoming subpaths is reflected, giving rise to independent fading multipath components. The total signal received at the BS for the kth user consists of L time delayed multipath replicas of the transmitted signal. The propagation channel for smart antenna system is shown in Fig. 1.

A. Channel Response Vector

For the given scenario, the channel impulse response between the lth multipath of the kth user and the nth antenna can be given as [13]

$$\begin{aligned} h_{k,l,n}(t) &= \sum_{s=1}^{S} \alpha_{k,l}^{(s)} \exp\left[-j\mathcal{K}d(n-1)\sin\theta_{k,l}^{(s)}\right]\delta(t-\tau_{k,l}) \\ &= \sqrt{\frac{\Omega_{k,l}}{S}} \sum_{s=1}^{S} \exp\left[j(\phi_{k,l}^{(s)} + 2\pi f_D\, t\cos\Psi_{k,l}^{(s)})\right] \\ &\quad \times \exp\left[-j\mathcal{K}d(n-1)\sin(\theta_k + \vartheta_{k,l}^{(s)})\right]\delta(t-\tau_{k,l}) \quad (1) \end{aligned}$$

where,
K is the total number of users (k is the user index);
L is the number of multipaths (l is the multipath index);
S is the number of sub-paths for each resolvable path which is assumed equal for different paths for simplicity (s is the subpath index);
N is the number of BS antennas (n is the antenna index);
d is the inter-element distance;
$\mathcal{K} = 2\pi/\lambda$ is the wave number;
$\delta(t)$ is the dirac delta function;
f_D is the Doppler frequency;
$\Omega_{k,l}$ is the mean path power of the lth multipath;
$\tau_{k,l}$ is the propagation delay of the lth multipath;
$\phi_{k,l}^{(s)}$ is random phase of each subpath;
$\Psi_{k,l}^{(s)}$ is the Angle of Departure (AOD) for each subpath relative to the motion of the mobile;
$\theta_{k,l}^{(s)} = \theta_k + \vartheta_{k,l}^{(s)}$, where θ_k is the mean Angle of Arrival (AOA);
$\vartheta_{k,l}^{(s)}$ is a zero mean random angular deviation with standard deviation σ_{AOA};
$\alpha_{k,l}^{(s)}$ denotes the complex subpath amplitude;

In vector notation, the spatial signature or channel response vector associated with the lth multipath of the kth user can be expressed by a $N \times 1$ vector as

$$\begin{aligned} \mathbf{h}_{k,l}(t) &= \Bigg[\sum_{s=1}^{S} \alpha_{k,l}^{(s)} \sum_{s=1}^{S} \alpha_{k,l}^{(s)} e^{[-j\mathcal{K}d\sin(\theta_k+\vartheta_{k,l}^{(s)})]} \\ &\quad \cdots \sum_{s=1}^{S} \alpha_{k,l}^{(s)} e^{[-j\mathcal{K}d(N-1)\sin(\theta_k+\vartheta_{k,l}^{(s)})]} \Bigg]^T \delta(t-\tau_{k,l}) \end{aligned} \quad (2)$$

B. LOS versus NLOS

In (1), the amplitude of the channel coefficients obeys Rayleigh distribution due to superposition of the subpaths. For the case of Rician fading, a direct Line Of Sight (LOS) component is added to the first multipath component with the shortest delay. The channel impulse response for the 1st resolvable multipath of the kth user at the nth antenna is given as

$$h_{k,1,n}(t) = \sqrt{\frac{K_R}{1+K_R}}\, h_{k,1,n}^{(LOS)}(t) + \sqrt{\frac{1}{1+K_R}}\, h_{k,1,n}^{(NLOS)}(t) \quad (3)$$

where K_R is the Rician factor defined as the ratio of the specular power to the scattered power (expressed in dB), $h_{k,1,n}^{(NLOS)}(t)$ is the scattered component given by (1) and $h_{k,1,n}^{(LOS)}(t)$ is the specular component given by

$$\begin{aligned} h_{k,1,n}^{(LOS)}(t) &= \exp\left[j(\phi_{k,1}^{(LOS)} + 2\pi f_D\, t\cos\theta_k)\right] \\ &\quad \times \exp\left[-j\mathcal{K}d(n-1)\sin\theta_k\right] \end{aligned} \quad (4)$$

where $\phi_{k,1}^{(LOS)}$ is the random phase of the LOS subpath.

C. System Model

Using (2), the received signal for the case of frequency selective fading can be written as

$$\mathbf{r}(t) \quad = \quad \sum_{k=1}^{K} \sum_{l=1}^{L} \mathbf{h}_{k,l}(t) x_k(t - \tau_{k,l}) + \mathbf{n}(t) \qquad (5)$$

where $\mathbf{r}(t)$ is $N \times 1$ received signal vector, $x_k(t)$ is kth user's transmitted signal and $\mathbf{n}(t)$ is $N \times 1$ Additive White Gaussian Noise (AWGN) vector.

III. Description of Channel Parameters

The spatial and temporal parameters of the channel model are described in more detail in this section.

1. Mean AOA

The K users are assumed be uniformly distributed in the sector over the azimuth range $[-60^\circ,\ 60^\circ]$. This assumption is made for simplicity and more complex distributions can also be adopted [14]. Each MS's incoming signal at the BS is described with a mean Angle of Arrival (AOA) θ_k. It is assumed that the AOA is the same for all the multipaths of a particular user, i.e. the spatial channel is assumed to be based on one AOA only ($\theta_{k,l} = \theta_k$) [2]. As per convention, the mean AOA θ_k is measured from the array broadside with $\theta = 0^\circ$ referred to as the broadside direction.

2. Fading Coefficients

The signal transmitted by the MS illuminates the local scattering structures around the MS. This generates numerous subpaths of the signal. The constructive and destructive combination of these randomly delayed, reflected, scattered and diffracted subpath signal components over distances of the order of a few wavelengths gives rise to fast fading. The Rayleigh distribution is used to model the fast fading in Non-Line-Of-Sight (NLOS) fading environments while the Rice distribution is used to model the fast fading when there is one direct Line-Of-Sight (LOS) component in addition to many random weaker NLOS components. In this work, the slow fading effects such as path loss and shadowing are not considered for simplicity but can easily be included in the channel model.

3. Power Delay Profile

The subpaths reach the BS either directly (line-of-sight propagation) or after undergoing further reflection from a dominant reflector (non-line-of-sight propagation), which gives rise to multipath propagation. We assume the dominant reflectors are significantly separated and a different combination of the incoming subpaths is reflected at each reflector. Thus each propagation path is associated with its own power and time delay. This information about the multipath delays ($\tau_{k,l}$) and powers ($\Omega_{k,l}$) is specified represented using the channel's Power Delay Profile (PDP), e.g. two or three ray power delay profiles [15]. Following [9], we assume that the time delays associated with the different resolvable multipaths are independent of the Angles of Arrival (AOA's).

4. PDF in AOD

The Probability Density Function (PDF) in the AOD at the MS describes the angular distribution of the subpaths departing the MS in azimuth. For the scenario considered in this work, it is assumed that the azimuth field distribution at the MS can be modelled by a uniform probability density function over $[0, 2\pi]$. This corresponds to the isotropic scattering model [16]. The model can also be easily extended to von Mises distribution, which includes uniform distribution as a special case and can also model nonuniform angular distribution of the subpaths at the MS [17].

5. PDF in AOA

The PDF in the AOA at the BS describes the angular distribution of the subpaths arriving at the BS in azimuth. It is assumed that the azimuth field distribution at the BS can be modelled by a Gaussian or Laplacian probability density function [4].

6. Doppler Frequency

The relative motion between the transmitter and receiver causes an apparent shift in the frequency of the received signal due to the Doppler shift. The Doppler shift is different for every subpath as it depends on the Angle of Departure (AOD) of the subpath relative to the direction of movement of the MS [16]. The maximum Doppler shift that the signal undergoes is $f_D = \frac{v}{\lambda} = \frac{v f_c}{c}$, where v is the vehicle speed (in m/s), λ is the wavelength of the transmitted signal, c is the velocity of light and f_c is the carrier frequency, e.g. a maximum Doppler frequency of 100 Hz corresponds to a speed of $v = 54$ km/hr for $f_c = 2$ GHz (i.e. a fast vehicular channel).

IV. Mobility Model

In order to simulate the effect of MS mobility, the following simulation strategy is adopted:-

- A 'drop' [9] is defined as the time required by the desired user to traverse the entire azimuth range $[-60^\circ, 60^\circ]$ with mean angle change $\Delta\theta$ per snapshot. The value of step size used is $\Delta\theta = 0.01^\circ$ per snapshot. This corresponds to an angular speed of 48 degree/s and provides a worst case scenario for a very fast moving MS at a very close distance to the BS, e.g. an MS travelling at velocity 300 km/hr at only 100 m from the BS [18], [19].
- At the beginning of each drop, the desired user's AOA is set to -60°, while the AOA's of the interferers are uniformly randomly distributed over the azimuth sector range.
- During a drop, a MS's AOA increases or decreases linearly with angle change $\Delta\theta$. Also the channel undergoes fast fading according to the motion of the MS's. The number of multipaths, number of subpaths and subpath parameters (angles of departures, random phases and angular spread) are kept constant as the mobile moves i.e. only the mean AOA θ_k of the path is adjusted as the mobile moves [10]. Additional randomness can also be introduced within each drop by "birth-death" technique of multipath generation [11].

The above mobility model ensures that the figure of merit used in the simulations (e.g. bit error rate) is averaged over

the ensemble of channel parameters and is not conditioned on a particular spatial or temporal state of the system [20].

V. Results

The results in this section are obtained by implementing the proposed channel model, using the MATLAB simulation model developed for the purpose [13]. The number of subpaths per path is $S = 20$, which is the value supported in the SCM specifications [9]. For simplicity, the case of $K = L = 1$ and single drop is considered here in order to study the properties of the simulated channel coefficients. Since all paths are assumed independent, the fading coefficients for additional users and multipaths can be generated by resetting the MATLAB random number generator seeds [13]. The main parameters used in the channel simulations are summarized in Table I.

TABLE I
Main Channel Simulation Parameters

Parameter	Value
No. of subpaths	$S = 20$
Doppler frequency	$f_D = 100$ Hz
Fading distributions	Rayleigh or Rician
Antenna geometry	Uniform linear array
Element pattern	Omnidirectional
Inter-element distance	$d = \lambda/2$
No. of BS antenna elements	$N = 1 - 8$
Angle of Arrival	$-60^\circ \leq \theta \leq 60^\circ$
User mobility	0.01° per snapshot
PDF in AOD	Uniform
PDF in AOA	Gaussian
Angle spread	$\sigma_{AOA} = 0^\circ, 10^\circ$

A. PDF of Channel Amplitudes

First, we investigate the temporal properties of the simulated channel. Fig. 2 shows the magnitude of the channel response using (3) for a total time period of $t = 100$ ms and Rician factors $K_R = -\infty, 5$ (dB). The curve for $K_R = -\infty$ dB corresponds to the case of Rayleigh fading. It can be seen that the signal fading is more severe with deeper and more frequent nulls for Rayleigh fading and this type of fading represents worst case channel for smart antennas.

We also compare the distribution of the channel coefficients with the theoretical prediction in order to check the accuracy of the simulated model. Fig. 3 shows the probability density histogram of the channel amplitudes for $K_R = -\infty$ and 5 dB. The ideal Rayleigh and Rician probability density functions are also shown for comparison. It can be seen that there is a very good match between the simulated and theoretical values. This shows that the proposed model is able to accurately simulate Rayleigh and Rician fading characteristics.

B. Space Time Fading

Next, we investigate the spatial properties of the simulated channel. Fig. 4 shows the channel magnitude response across a $N = 8$ ULA with inter-element spacing $d = \lambda/2$, over a period of 40 ms with Doppler frequency $f_D = 100$ Hz, mean AOA $\theta = 0^\circ$ and angle spread $\sigma_{AOA} = 10^\circ$. From the figure it can be seen that the channel coefficients at different antennas at a particular time instant have different magnitude i.e. there is spatial fading across the array as a consequence of non-zero angle spread. This is because the different subpaths contributing to the received signal arrive from different directions and their relative phase shifts are different, and therefore, they add up either constructively or destructively at each point across the array depending on the relative phase relationship. This produces space-time selective fading.

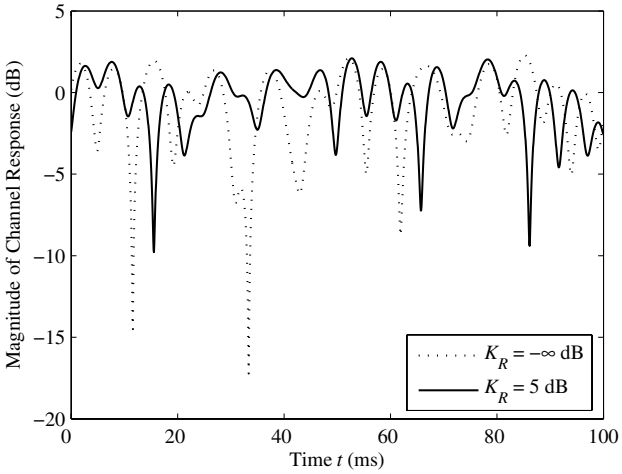

Fig. 2. Channel magnitude response for single antenna assuming Doppler frequency $f_D = 100$ Hz, mean AOA $\theta = 0^\circ$, Rician factor $K_R = -\infty, 5$ dB and no angle spread.

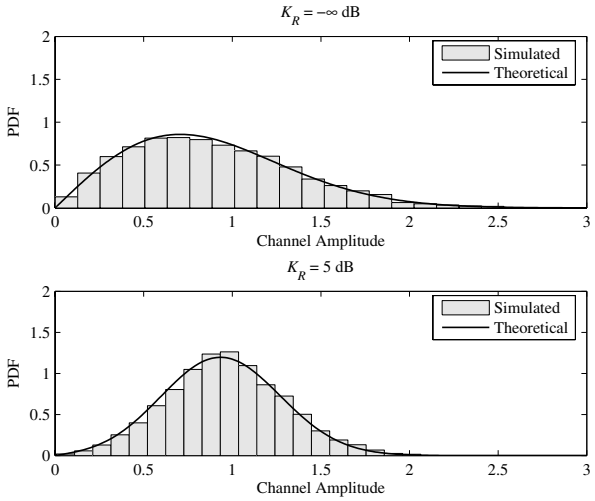

Fig. 3. The probability density histograms of the channel amplitude assuming Rician fading and Rice factors $K_R = -\infty, 5$ dB.

C. Model Validation

The proposed model can be applied to link-level simulations for adaptive antenna applications, e.g. the model was used to generate the channel coefficients in the simulation model for a CDMA smart antenna system in [20], where it was shown to provide very good agreement with theoretical results.

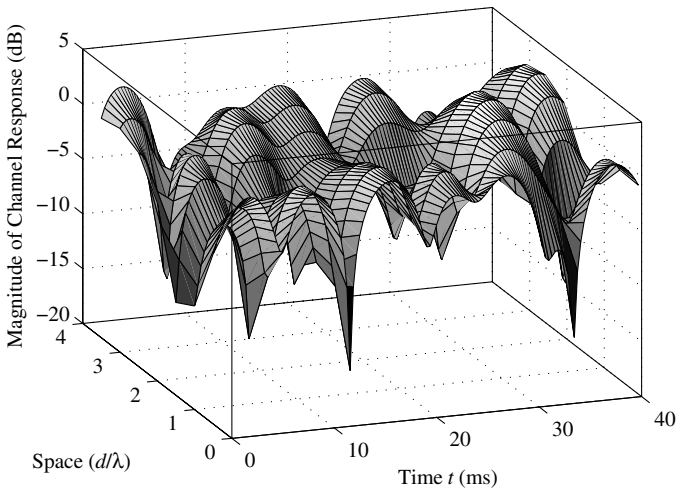

Fig. 4. Space-time fading: $N = 8$ antenna elements, $d = \lambda/2$, Doppler frequency $f_D = 100$ Hz and angle spread $\sigma_{AOA} = 10^\circ$.

VI. Conclusions

In this paper, we have presented a parameterized physical channel model for use in performance evaluation of smart antenna systems. The model is general and flexible to include different propagation aspects such as fading distributions, array geometry, angle spread, power delay profiles and Doppler frequency. The model also provides a comprehensive framework for inclusion of mobile station mobility. A mathematical formulation of the channel model has been presented, along with the simulation results. The obtained results have shown that the simple model can accurately characterise different channel environments for smart antennas.

References

[1] A. Alexiou and M. Haardt, "Smart antenna technologies for future wireless systems: trends and challenges," *IEEE Commun. Mag.*, vol. 42, no. 9, pp. 90–97, Sept. 2004.

[2] R. Ertel, P. Cardieri, K. W. Sowerby, T. S. Rappaport, and J. H. Reed, "Overview of spatial channel models for antenna array communication systems," *IEEE Personal Commun. Mag.*, vol. 5, no. 1, pp. 10–22, Feb. 1998.

[3] K. Yu and B. Ottersten, "Models for MIMO propagation channels: A review," *Wireless Communications and Mobile Communications*, vol. 2, no. 7, pp. 653–666, Nov. 2002.

[4] K. Pedersen and P. Mogensen, "A stochastic model of the temporal and azimuth dispersion seen at the base sation in outdoor propagation environments," *IEEE Trans. Veh. Technol.*, pp. 437–447, Mar. 2000.

[5] K. Rizk, J.-F. Wagen, and F. Gardiol, "Two-dimensional ray-tracing modeling for propagation prediction in microcellular environments," *IEEE Trans. Veh. Technol.*, vol. 46, no. 2, pp. 508–518, May 1997.

[6] P. Petrus, J. H. Reed, and T. S. Rappaport, "Geometrically based statistical channel model for macrocellular mobile environments," in *Proc. IEEE Global Telecommunications Conference (GLOBECOM)*, London, UK, Nov. 1996, pp. 1197–1201.

[7] R. Janaswamy, "Angle and time of arrival statistics for the gaussian scatter density model," *IEEE Trans. Wireless Commun.*, vol. 1, no. 3, pp. 488 –497, July 2002.

[8] H. Xu, D. Chizhik, H. Huang, and R. Valenzuela, "A generalized space-time multiple-input multiple-output (MIMO) channel model," *IEEE Trans. Wireless Commun.*, vol. 3, no. 3, pp. 966–974, May 2004.

[9] Third Generation Partnership Project Two (3GPP2), "Spatial Channel Model for Multiple Input Multiple Output (MIMO) simulations (3GPP TR 25.996)," Sept. 2003.

[10] J. Jelitto, M. Stege, M. Lohning, M. Bronzel, and G. Fettweis, "A vector channel model with stochastic fading simulation," in *Proc. IEEE International Symposium on Personal, Indoor and Mobile Radio Communications (PIMRC)*, Osaka, Japan, Sept. 1999.

[11] R. J. Piechocki and G. V. Tsoulos, "A macrocellular radio channel model for smart antenna tracking algorithms," in *Proc. IEEE Vehicular Technology Conference (VTC)*, Houston, Texas, May 16-20, 1999, pp. 1754–1758.

[12] L. Correia, Ed., *Wireless Flexible Personalised Communications - COST 259 Final Report*. John Wiley & Sons, 2001.

[13] S. Durrani, "Investigation into smart antennas for CDMA wireless systems," Ph.D. dissertation, The University of Queensland, Brisbane, Australia, Aug. 2004.

[14] M. Lotter and P. V. Rooyen, "Modelling spatial aspects of cellular CDMA/SDMA systems," *IEEE Commun. Lett.*, vol. 3, no. 5, pp. 128–131, May 1999.

[15] A. Paulraj, R. Nabar, and D. Gore, *Introduction to Space-Time Wireless Communications*. Cambridge Univ. Press, 2003.

[16] W. C. Jakes, *Microwave Mobile Communications*. John Wiley, 1974.

[17] A. Abdi, J. A. Barger, and M. Kaveh, "A parametric model for the distribution of the angle of arrival and the associated correlation function and power spectrum at the mobile station," *IEEE Trans. Veh. Technol.*, vol. 51, no. 3, pp. 425–433, May 2002.

[18] Y. S. Song, H. M. Kwon, and B. J. Min, "Computationally efficient smart antennas for CDMA wireless communications," *IEEE Trans. Veh. Technol.*, vol. 50, no. 6, pp. 1613–1628, Nov. 2001.

[19] T. Ihara, S. Tanaka, M. Sawahashi, and F. Adachi, "Fast two-step beam tracking algorithm of coherent adapative antenna array diversity receiver in W-CDMA reverse link," *IEICE Transactions on Communications*, vol. E84-B, no. 7, pp. 1835–1848, July 2001.

[20] S. Durrani and M. E. Bialkowski, "Analysis of the error performance of adaptive array antennas for CDMA with noncoherent M-ary orthogonal modulation in Nakagami fading," *IEEE Commun. Lett.*, vol. 9, no. 2, pp. 148–150, Feb. 2005.